Journal of Petroleum Science and Engineering 175 (2019) 1112–1121

Contents lists available at ScienceDirect

Journal of Petroleum Science and Engineering

journal homepage: www.elsevier.com/locate/petrol

Characteristics and formation mechanism of natural fractures in the tight gas sandstones of Jiulongshan gas field, China

Lei Gong[a], Xiaocen Su[a], Shuai Gao[a,*], Xiaofei Fu[a], Hadi Jabbari[b], Xixin Wang[c,**], Bo Liu[d], Wenting Yue[e], Zhaosheng Wang[f], Ang Gao[g]

[a] College of Geosciences, Northeast Petroleum University, Daqing, 163318, Heilongjiang, China
[b] Petroleum Engineering Department, University of North Dakota, Grand Forks, 58202, North Dakota, USA
[c] College of Geosciences, China University of Petroleum-Beijing, Beijing, 102249, China
[d] Institute of Unconventional Oil & Gas, Northeast Petroleum University, Daqing, 163318, Heilongjiang, China
[e] Department of Overseas Strategy & Production Planning Research in CNPC International Research Center, Beijing, 100083, China
[f] College of Mining Engineering, North China University of Science and Technology, Tangshan, 063210, Hebei, China
[g] The Fourth Oil Production Company of Daqing Oil Field Co. Ltd., Daqing, 163511, Heilongjiang, China

ARTICLE INFO

Keywords:
Tight gas sandstone
Natural fractures
Fracture characteristics
Formation mechanism
Jiulongshan gas field

ABSTRACT

Natural fractures control the migration and accumulation of oil and gas in the tight sandstones. Understanding the characteristics and formation mechanism of natural fractures has important guiding significance to the comprehensive prediction and evaluation of the fracture distribution. Focusing on the tight sandstones of the Xujiahe Formation (T_3x) of Jiulongshan gas field, northwest Sichuan Basin, China, the characteristics of natural fractures were characterized quantificationally, and a comprehensive evaluation method of fracture formation mechanism is proposed. Two types of natural fractures were identified in the T_3x, namely tectonic fractures and diagenetic fractures. Most of the natural fractures are tectonic shear fractures, which can be subdivided into steep fractures and nearly horizontal fractures according to their dip angles. Three sets of tectonic fractures were identified in the study area, namely: NW-SE trending, NNE-SSW trending and NEE-SWW trending fractures. According to the characteristics of fracture sets, crosscutting relationships, acoustic emission tests and fluid inclusion analysis, and combined with the tectonic evolution history of the study area, the natural fractures were formed in four periods. Among them, the diagenetic fractures formed at the process of diagenesis are the first period fractures. The second to fourth periods are tectonic fractures formed at the end of the Triassic to the Early Jurassic, the Late Cretaceous and the end of Pliocene to the early of Pleistocene, respectively. Horizontal tectonic compression, uplift denudation and overpressure were the main force sources for the formation of the steep tectonic fractures. The formation of nearly horizontal fractures is related with the thrusting or inter-formational sliding caused by tectonic compression.

1. Introduction

Natural fracture system is the key factor in controlling the migration, accumulation and high output of hydrocarbons in tight sandstone reservoirs (Laubach et al., 2010; Olson et al., 2010; Luo et al., 2018; Wang et al., 2018a,b). The viewpoint of “no fracture, no hydrocarbon accumulation” has been put forward for many tight oil and gas fields (Zeng and Li, 2010; Lyu et al., 2016; Kong et al., 2018). Research on the spacial distribution characteristics of natural fractures is becoming indispensable for the exploration of these tight oil and gas reservoirs (Sanderson and Nixon, 2015; Zhao et al., 2018; Wang et al., 2018a,b).

The Jiulongshan gas field is a large gas bearing anticline, which is located at the northwest Sichuan Basin, China (Fig. 1). The explorations have proved that the Xujiahe Formation (T_3x) of the Jiulongshan gas field has promising natural gas resource potential with a tremendous exploration prospect (Qiu and He, 1990; He et al., 1999; Liu et al., 1996). However, the existing research shows that the sandstones of the Xujiahe Formation (T_3x) are very tight, whose matrix porosity is generally less than 7.0% and more than 98% of the matrix permeability is less than 0.1 mD. The natural fracture system controls the enrichment and production of natural gas (Pei et al., 2008; Zeng, 2010; Bai et al., 2012; Lyu et al., 2017). More research on the characteristics and

* Corresponding author.
** Corresponding author.
E-mail addresses: 349684871@qq.com (S. Gao), 287755674@qq.com (X. Wang).

https://doi.org/10.1016/j.petrol.2019.01.021
Received 9 August 2018; Received in revised form 13 December 2018; Accepted 3 January 2019
Available online 04 January 2019

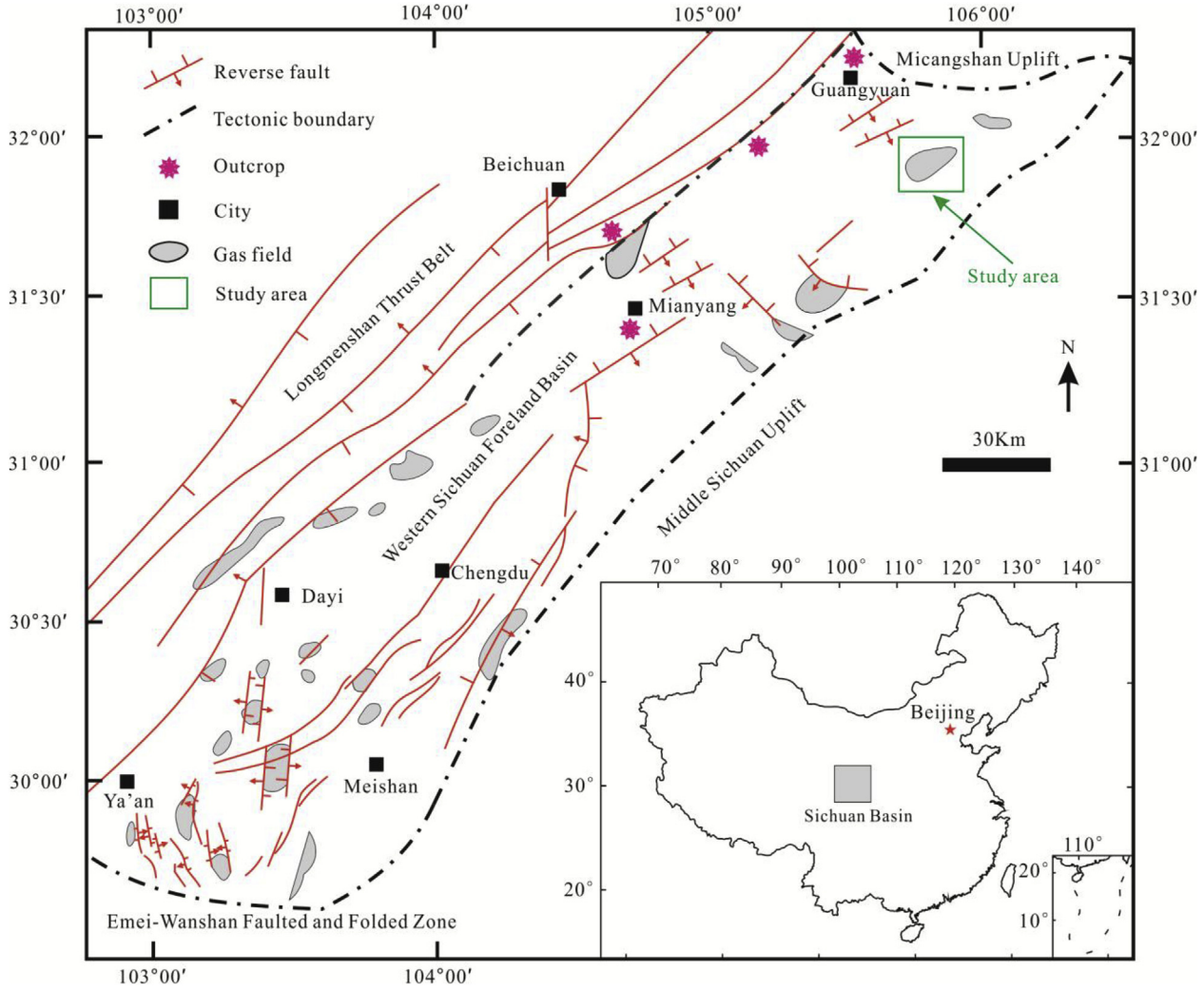

Fig. 1. Tectonic outline map of the western Sichuan Basin and the location of the Jiulongshan gas field, China (Modified from Gong et al., 2016).

genetic mechanism of natural fractures in Jiulongshan gas field can improve the prediction of fractures distribution in this tight reservoir which leads to more gas exploration in this field (Larsen et al., 2010; Ferrill et al., 2014; Laubach et al., 2016).

Previous studies analyzed the paleo-tectonic stress field of northwestern Sichuan Basin and confirmed that this area mainly experienced three periods of tectonic event: late Indosinian period, late Yanshan period, and Himalayan period, respectively (Liu et al., 1994; Cao, 2005; Yuan et al., 2010). He et al. (1999) predicted the fracture distribution of Xujiahe Formation (T_3x) using data of mechanical properties and structural curvature. However, limited by scarce data, a comprehensive research on the fracture characteristics, sequences and formation mechanism is still lack, which is the basis for better understanding the occurrence and spacial distribution of the natural fractures. With the deepening of exploration, more core and log data are available in recent years. Based on data of cores, image logs, thin sections, outcrops and experiments, the types, characteristics, sequences and the formation mechanism of natural fractures in the Xujiahe Formation (T_3x) were investigated in this work.

2. Geological setting

The Jiulongshan gas field is a NE-SW trending dome shaped anticline, which is located at the intersection of the Longmenshan thrust belt and Micangshan uplift belt in the northwest of Sichuan Basin (Fig. 1). The Xujiahe Formation (T_3x) are divided into five Members (i.e., 1st to 5th Member) from bottom to top in the Western Sichuan Foreland Basin (Fig. 2). Among them, the 1st (T_3x^1), 3rd (T_3x^3) and 5th (T_3x^5) Members are the source rocks, and the 2nd (T_3x^2) and 4th (T_3x^4) Members are the reservoir rocks. However, due to the tectonic uplift in the late Indosinian period, the 4th (T_3x^4) and 5th (T_3x^5) Members are missing in the Jiulongshan gas field (Pei et al., 2008).

The burial depth of the Xujiahe Formation (T_3x) is generally more than 3100 m, and the thickness is about 280 m–310 m. The depositional environment is mainly of fan delta front. The lithology of the reservoir is mainly lithic feldspar sandstone, feldspar sandstone and quartz sandstone with fine to medium grains. The main porosity is comprised of intergranular pores and dissolution pores. There are several small-scale reverse faults with throw between 10 m and 100 m in the study area. Because the reservoir rocks are tight and brittle, the fractures are highly developed under the strong tectonism, which makes the reservoir to be a fractured reservoir.

3. Methods

Based data of 4 outcrops, 524 m cores from 16 wells, 154 thin sections, image logs from 5 wells and the relevant experiments, the features of natural fractures were characterized, and their formation mechanism was discussed. The fracture occurrence (strike and dip angle) was constrained by direct measure of fractures from outcrops using a geological compass and interpretation of image logs. Fractures were divided into sets according to their orientations, cross-cutting

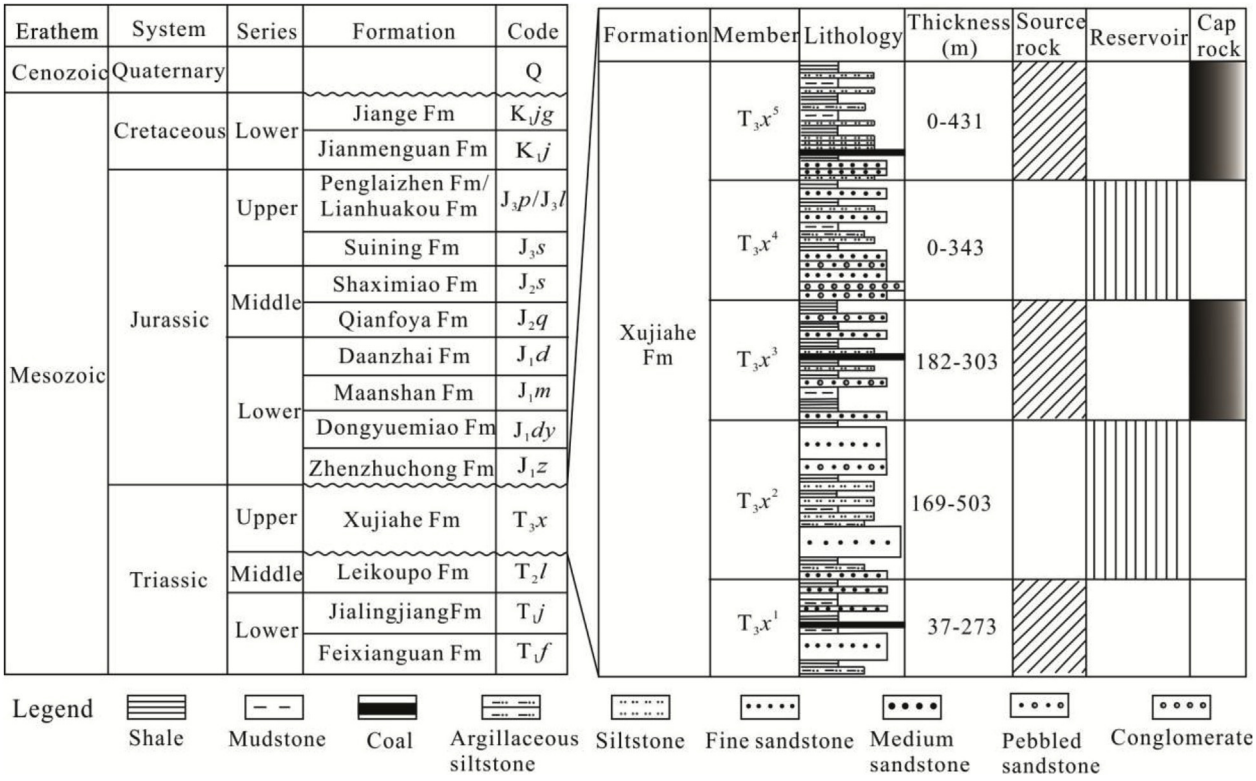

Fig. 2. Stratigraphic column of Western Sichuan Foreland Basin (Modified from Lyu et al., 2017). Fm = Formation.

relationships, and cement types. Fracture density was measured by correcting the scan lines parallel to the borehole using the Terzaghi's correction method (Casini et al., 2016; Marrett et al., 2018; Procter and Sanderson, 2018).

Acoustic emission is an elastic wave which is generated by a rapid release of strain energy stored in the material (Zeng and Li, 2010; Gong et al., 2017). In general, metals have memory of their stress history. Materials produce clear acoustic emissions when the stress reaches the maximum stress they have experienced, which is known as the Kaiser effect. In fact, numerous studies show that rocks also have good memory function with respect to the earlier stress (Ding and Zhang, 1991; Bai et al., 2012). A large number of micro-cracks were formed when the rock experienced multiple periods of paleo-tectonic stress. These micro-cracks expand when the stress imposed on the rock reaches the paleo-stress of each period that they have experienced, and many different Kaiser effect points is formed. Each Kaiser effect point represents one rupture event. Therefore, these Kaiser effect points can be used to estimate the rupture periods of rocks. In this study, acoustic emission (AE) features of 12 core plugs were measured using the PCI-2 acoustic emission detecting system at Northeast Petroleum University, which can help constraint the fracture events. These samples were processed into 25 mm * 50 mm (diameter * height) cylinders, which were flattened at both ends. To reduce the end effect, butter was applied at both ends of the sample. Acoustic emission probes were installed on the side of the samples. And then the sample was fixed on a servo mechanical testing machine and loaded by displacement control method. The loading rate was 0.002 mm/s until the sample was destroyed. The stress, strain and the number of acoustic emission were recorded during the experiment.

According to the characteristic analysis and homogenization temperature measurement of fluid inclusions contained within the fracture filling minerals, the paleo-temperature when the filling minerals formed can be obtained (Ferrill et al., 2017; Lyu et al., 2017). Combined with the burial history and geo-temperature history, the fracture formation sequence can be constrained. In this study, 14 samples containing fractured fillings were obtained from cores and processed into thin sections with thickness of 0.05 mm. Firstly, the morphology, size and color of fluid inclusions were observed under Leica 4P microscope. Then the homogenization temperature of selected fluid inclusions were measured by Linkam THMSG600 Cooling-Heating Stage. The homogenization temperature of totally 125 fluid inclusions were measured to help constraint the fracture sequences in this study.

4. Results

4.1. Fracture types

Both tectonic fractures and diagenesis fractures developed in the Xujiahe Formation (T_3x). The tectonic shear fractures are the main fracture type. They are widely distributed in multiple lithology types with a regular distribution and an obvious directivity, and often in groups (Fig. 3, Fig. 4). Tectonic fractures can be subdivided into steep fractures and nearly horizontal fractures according to their dip angles. The steep fractures usually show an en echelon array (Fig. 3A, B & C). Some of them were filled with minerals (mainly are calcite or quartz). The surfaces of these steep fractures are smooth and often characterized by slickensides and steps. The nearly horizontal fractures are mainly developed in medium sandstone and gritstone near the thrust faults or sliding layers (Fig. 3D). They usually have equal spacing, being 3 cm–5 cm. These horizontal fractures seem to be parallel to the bedding planes, but they actually intersect with the bedding planes at a small angle. Some of these horizontal fractures are filled with minerals or/and show signs of dissolution. In some core intervals, these nearly horizontal fractures are cut visibly by the steep fractures, or vice versa. These steep fractures and nearly horizontal fractures interlace together and form prolific fracture networks, making the wells drilled in those areas are very productive.

Diagenetic fractures usually develop along the bedding planes, especially along the lithologic interfaces, such as the interface between sandstone and mudstone (Fig. 5). Most of the tectonic fractures were

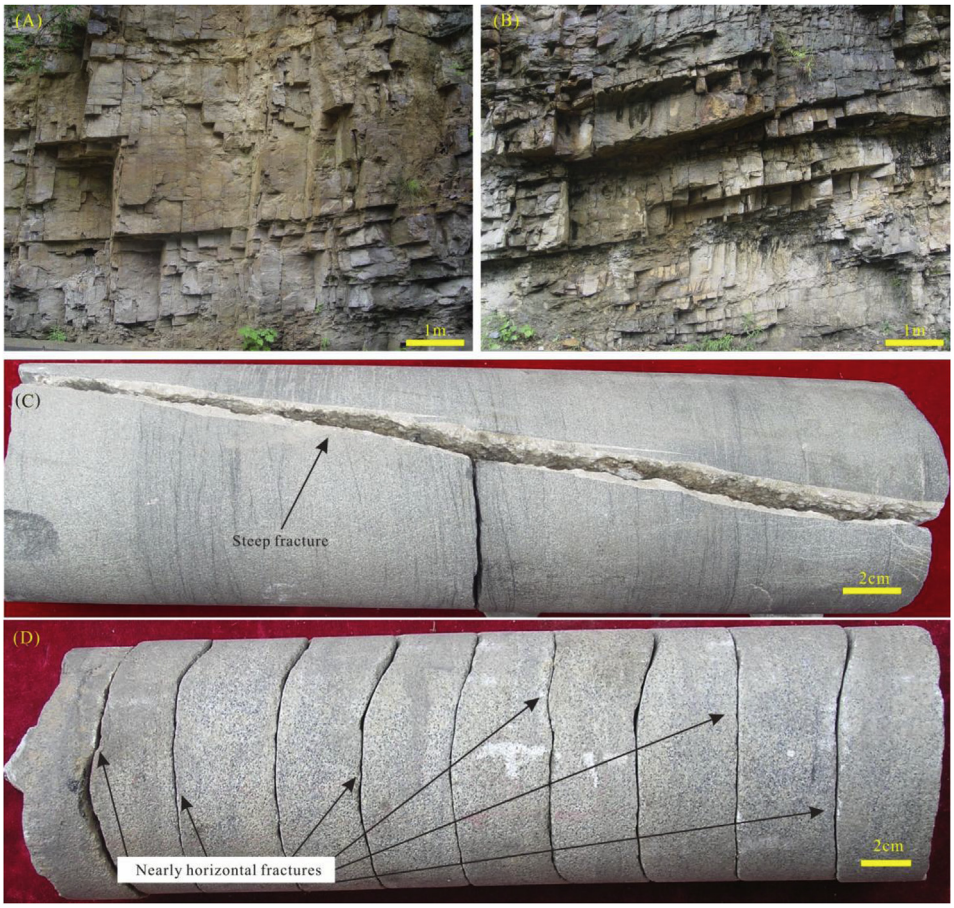

Fig. 3. Tectonic fractures in outcrops and cores. (A) and (B) Two sets of steep fractures from outcrops. (C) Steep tectonic fracture in core (filled with calcite). (D) Nearly horizontal fractures in core.

constrained by these bedding parallel diagenetic fractures (Petrie et al., 2014; Smart et al., 2014; Agosta et al., 2015). The bedding parallel fractures may show signs of interruption, bending, wedge-out, combining, or branching along the bedding plane which means that they were formed in the process of long-term evolution in the reservoirs. Although these bedding-parallel fractures are widely distributed, the extended length is limited, and because they are deep buried and nearly horizontal, they are generally closed under the lithostatic pressure of the overlying strata. Therefore, they present little contribution to the fluid flow in the reservoirs.

4.2. Logging responses of the natural fractures

Opening tectonic fracture result in local decrease of formation resistivity and local increase of acoustic impedance, thus the decrease of local echo amplitude. Therefore, they are shown as dark sinusoidal or cosine curves in both electrical and acoustic imaging maps. But the fractures are often partially filled with quartz, calcite or other minerals, which makes the formation resistivity and acoustic impedance decrease/increase unevenly. Therefore, there are intermittent or irregular changes in the dark sine or cosine curves (Fig. 4).

Conventional logging curves also respond to tectonic fractures (Ge et al., 2014, 2015; Lyu et al., 2016). By comparing the conventional logging curves of fractured and un-fractured sections, the gamma ray (GR) of fractured section is slightly reduced, the negative anomaly of spontaneous potential (SP) is increased, and the caliper (CAL) is slightly enlarged on the cross plot of lithologic indicator curves (Fig. 6A). On the cross plot of three porosity curves, the interval acoustic transit time (AC) of fractured section increases, the neutron porosity (CNL) varies slightly, and the density value (DEN) decreases slightly (Fig. 6B). On the cross plot of resistivity curve, the resistivity value of fractured section decreases slightly, and the difference of resistivity between deep resistivity (RT) and shallow resistivity (RXO) decreases slightly, which indicates that fractures reduce deep resistivity (Fig. 6C). However, the response of single log curve to fracture is very weak, so it is necessary to take corresponding measures to enhance the overall signal in order to reflect the development of fractures more clearly and accurately.

4.3. Fracture development characteristics

According to the interpretation of image logs and fracture occurrence measurements conducted on outcrops, three sets of fractures can be detected in the Xujiahe Formation (T_3x), namely: NW-SE trending, NNE-SSW trending, and NEE-SWW trending (Fig. 7). The dip angles of steep fractures are greater than 70°, while the dip angles of the nearly horizontal fractures are usually between 10° and 30°.

The fracture heights measured from cores and outcrops are mainly distributed between 20 cm and 50 cm, which indicates that most of the fractures are confined in a single layer. The average fracture density of the steep fractures is 0.58 m^{-1}, and it varies distinctly in different tectonic position and layers. In the vicinity of faults and hinges of folds, fracture density increases significantly due to an intense stress disturbance caused by faulting and folding. The highest average fractures density in a single well can be as high as 1.23 m^{-1}. Furthermore, there exists different fracture development degrees in the vertical direction. Fractures are most developed in the upper of the Xujiahe Formation with an average fracture density of 0.71 m^{-1}. The middle of the Xujiahe Formation is the second most developed layer with an average fracture

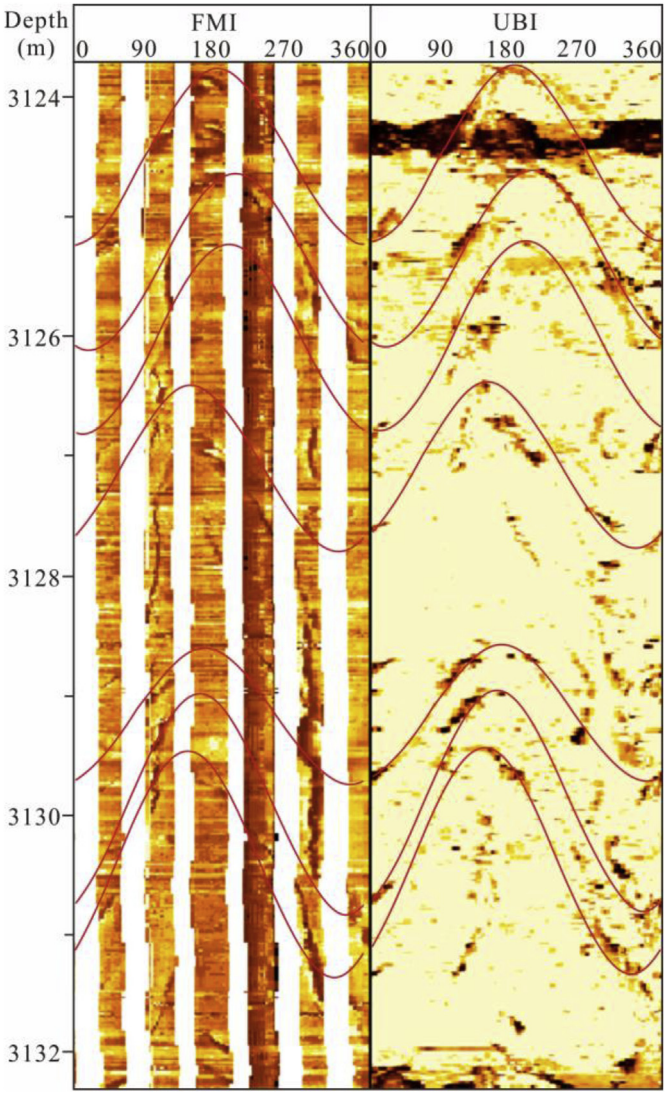

Fig. 4. Natural steep fractures detected from electrical and sonic image logs. FMI = Fullbore Microscan Imager, UBI = Ultra Borehole Imager.

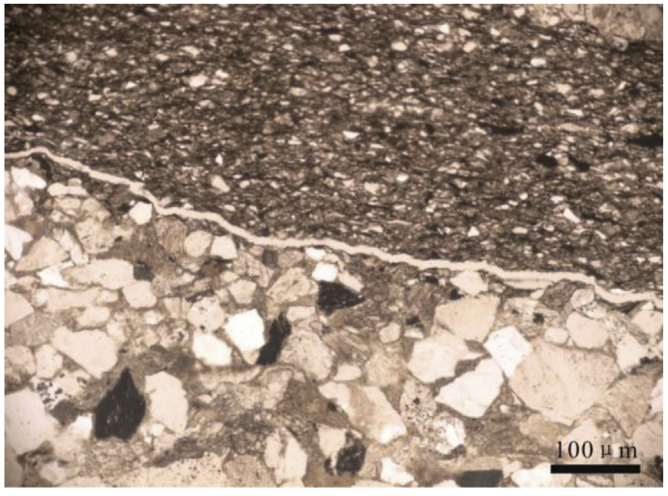

Fig. 5. Diagenetic fractures in thin-section.

density of 0.56 m^{-1}, while the fracture density is the smallest in the lower of the Xujiahe Formation, i.e. only about 0.42 m^{-1}. Such a change in fracture density should be related to the difference of their lithology and bed thickness (Laubach et al., 2009; Ameen et al., 2012; Hooker et al., 2013; Gong et al., 2015).

4.4. Crosscutting relationships

The filling minerals in the fractures mainly include quartz, calcite and carbonaceous clay. Among them, the carbonaceous clay is usually filled in the bedding parallel diagenetic fractures while the quartz and calcite are filled in the tectonic fractures. According to the fracture crosscutting relationships (Fig. 8), three phenomena can be observed: (1) calcite cuts calcite (fractures filled with calcite cut those filled with calcite); (2) quartz cuts calcite; c) calcite cuts quartz. Among them, the first phenomenon reflects that the fractures experienced two periods of calcite filling events. The second phenomenon reflects the fractures experienced one period of calcite filling event and one period of quartz filling event separately, and the calcite filling preceded the quartz filling. The third phenomenon happened when the fractures experienced one period of calcite filling event and one period of quartz filling event, with quartz preceding the calcite filling.

According to the above analysis, four stages of filling events can be identified: first, the carbonaceous clay filled in the nearly horizontal diagenetic fractures. Next, calcite filled in the tectonic fractures. Then, quartz filled in the tectonic fractures. Finally, calcite filled in the tectonic fractures.

In the outcrops, three sets of fractures were identified. Among them, the NNE-SSW trending fractures usually abut at the NW-SE trending fractures, while the NEE-SWW trending fractures abut at the NNE-SSW trending fractures (Fig. 9), which indicates that the NW-SE trending fractures are the first period of fractures, the trending NNE-SSW fractures are the second period of fractures, and the NEE-SWW trending fractures are the third period of fractures.

4.5. Acoustic emission test

The acoustic emission test results of 12 core plug samples from the Xujiahe Formation (T_3x) show that, almost all of the 12 samples present 4 Kaiser effect points (Table 1), which indicates that these core samples mainly experienced 4 micro-rupture events, and the maximum principal stresses of these 4 micro-rupture events were 82.4 MPa, 93.0 MPa, 103.5 MPa and 112.4 MPa, respectively. Among them, the fourth Kaiser effect point (red point in Fig. 10) is caused by the final breakdown of the core sample during the acoustic emission test, while other three Kaiser effect points (green points in Fig. 10) represent the three micro-rupture events that the core samples have experienced.

4.6. Homogenization temperature of fluid inclusions

Based on the homogenization temperature measurements of fluid inclusions of 14 quartz or calcite samples cemented in the tectonic fractures of the study area (Fig. 11), their homogenization temperature ranges from 60 °C to 150 °C and can be divided into three sets with homogenization temperatures of 70 °C–80 °C, 90 °C–100 °C and 130 °C–140 °C, respectively. Therefore, three crack-sealing events can be determined, which reflects three fracture events. Combined with the burial history and geo-temperature history, the three crack-sealing events were at the Early Jurassic, the Late Cretaceous and the end of Pliocene to the early of pleistocene, respectively (Fig. 12).

5. Discussion

5.1. Fracture sequence

The formation sequence and time of natural fractures are very

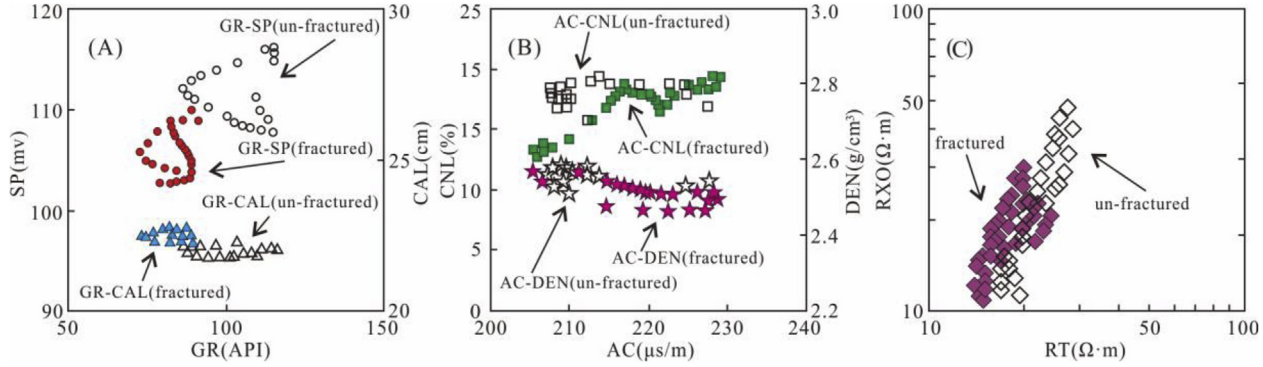

Fig. 6. Cross plot of (A) lithology curves, (B) porosity curves and (C) resistivity curves of fractured and un-fractured sections.

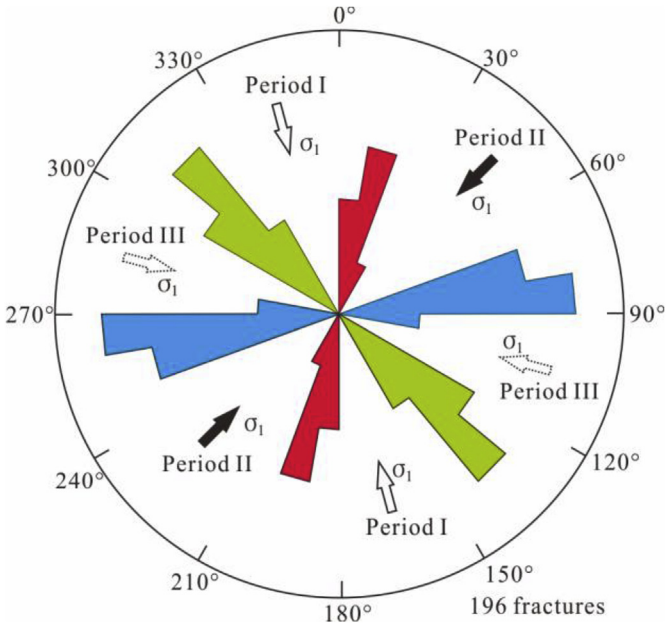

Fig. 7. Sets and strikes of tectonic fractures and their relationships with the paleo-stresses in the Xujiahe Formation (T_3x) of Jiulongshan gas field (Modified from Gong et al., 2013).

important for the role of fractures in hydrocarbon accumulation. Fracture sets division and crosscutting relationship can qualitatively judge the formation sequence of different sets of fractures, but the specific fracture formation time can't be determined. Fluid inclusion analysis can help to define the latest stage of fracture formation, but the time between fracture formation and mineral deposition is difficult to determine. Rock acoustic emission data can be used to estimate the time and intensity of Paleo-tectonic stress, but local tectonic events and rock heterogeneity may affect its accuracy. Therefore, it is necessary to combine the tectonic evolution history of the study area and synthesize these methods to determine the sequence and time of fracture formation.

Former researchers analyzed the paleo-tectonic stress field with the consideration of structural features along with sedimentary and joint analyses (Liu et al., 1994; Cao, 2005; Yuan et al., 2010). Based on their evaluations, three sets of structural lineaments developed in this area, namely NNE-SSW trending, NEE-SWW trending and NW-SE trending. According to their crosscutting relationships, the NEE-SWW structural lineament formed relatively early, the NNE-SSW structural lineament formed relatively late while the NW-SE structural lineament formed between the two sets mentioned above. The formation time of these three sets of structural lineaments were the end of Late Triassic, the Late Cretaceous and the end of Pliocene to the early of Pleistocene, respectively.

Based on the above characteristics of fracture sets, crosscutting relationships, and results of acoustic emission experiments and fluid inclusions, and combined with the tectonic evolution of the northwest Sichuan Basin (Liu et al., 1994; Cao, 2005; Yuan et al., 2010), four periods of fractures can be identified in the study area (Fig. 13). The first period is the diagenetic fractures. These diagenetic fractures formed under the intense compaction and dissolution, the formation time is from Late Triassic to Early Cretaceous. All the other three periods of fractures are tectonic fractures. Among them, the first period of tectonic fractures formed under the tectonic compression of Indosinian movement at the end of the Triassic to the Early Jurassic. The second period of tectonic fractures formed under the influence of abnormal high pressure and tectonic compression at the Late Cretaceous. The third period of tectonic fractures formed under strong tectonic uplift and denudation between the end of Pliocene and the early of Pleistocene.

5.2. Fracture formation mechanism

Jiulongshan area experienced the NNW-SSE horizontal tectonic compression and uplift denudation caused by the Longmen mountain at the end of Triassic. The tectonic compression increases the maximum principal stress, and the denudation decreases the minimum principal stress, both of which make the Mohr circle larger and intersect with the failure envelop (Fig. 14A). Therefore, under these conditions, rocks may easily rupture in the Xujiahe Formation (T_3x) where leads to the formation of NNE-SSW and NW-SE trending fractures (Fig. 7). At late Cretaceous, the study area was subjected to the NE-SW horizontal tectonic compression from the Micangshan tectonic belt. At the same time, the buried depth of the Xujiahe Formation (T_3x) reached a maximum, and an abnormal high fluid pressure formed (Liu et al., 1994). The presence of the abnormally high fluid pressure reduces the maximum and minimum principal stress simultaneously, which make the Mohr circle move to the left and thus intersects with the failure envelop (Fig. 14B). Under these combined effects from horizontal tectonic compression and the high abnormal fluid pressure, the NEE-SWW and NNE-SSW trending fractures formed (Fig. 7). At end of Pliocene to the early of Pleistocene, under the lateral tectonic compression from the Qinghai-Tibet plateau, the Longmenshan thrust belt reactivated which put the study area under NWW-SEE horizontal tectonic compression and uplift denudation, and thus the NE-SW and NEE-SWW trending fractures formed (Fig. 4A and C, Fig. 7).

About the origin of those nearly horizontal fractures, some viewpoints exist: unloading while tectonic uplift, stress disturbance caused by coring and tectonic shearing (Yu and Zhou, 2001; Zeng et al., 2012). These fractures with low dip angle distributed nearly parallel to the bedding plane, but not along the bedding plane, meaning that they are not bedding fractures caused by unloading in the process of coring. Also, these fractures have characteristics of shear fractures, for example

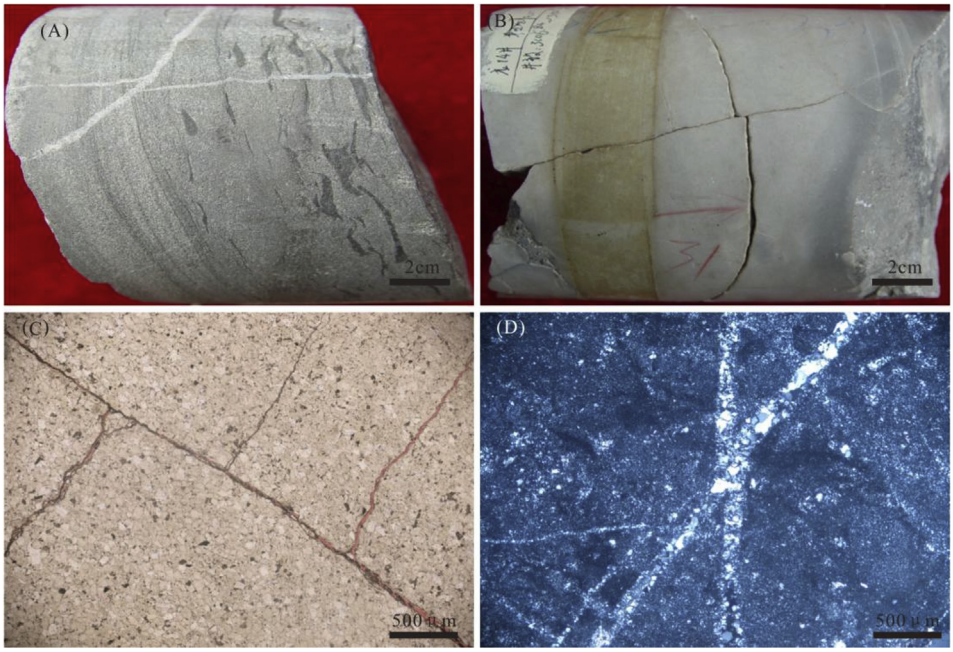

Fig. 8. Fracture crosscutting and abutting relationships in the Xujiahe Formation (T_3x) of Jiulongshan gas field.

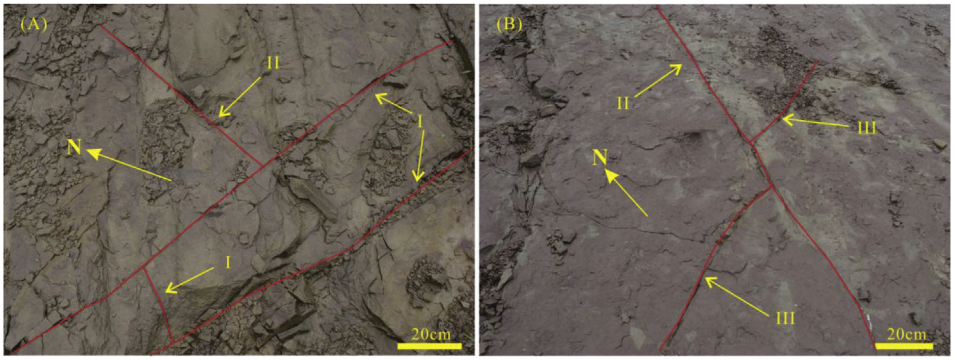

Fig. 9. Abutting relationships of different sets of fractures from outcrops.

Table 1
Stress data measured from the acoustic emission tests of 12 core samples from Xujiehe Formation (T_3x) of Jiulongshan gas field (Gong et al., 2013).

No.	Stress (MPa)							
	75–80	80–85	85–90	90–95	95–100	100–105	105–110	110–115
L10-1	75.6	82.0	85.0	–	–	103.4	–	–
L10-2	–	–	–	–	–	102.5	–	112.4
L10-3	–	82.5	–	93.6	97.3	–	106.1	–
L10-4	–	83.2	–	91.9	–	104.3	–	111.5
L10-5	78.8	83	88.6	91.6	–	–	–	–
L10-6	–	84.2	–	–	–	104.9	–	110.6
L14-1	75.0	–	–	92.9	–	–	–	112.5
L14-2	77.8	81.6	86.5	–	–	104.2	–	–
L14-3	–	–	–	94.6	–	103.5	–	113.4
L14-4	–	82.1	–	92.1	96.5	–	110.4	114.7
L14-5	–	–	–	94.6	–	101.4	–	111.5
L14-6	–	80.9	–	–	–	–	112.6	–
Frequency	33.3%	66.7%	25.0%	58.3%	33.3%	58.3%	25.0%	58.3%
Average stress	–	82.4	–	93.0	–	103.5	–	112.4

there are slickensides on the fracture surface and they cut through rock grains. These nearly horizontal fractures should be natural tectonic shear fractures formed in the tectonic movement, and their formation is mainly related with the thrusting or inter-formational sliding caused by tectonic compression.

6. Conclusion

Both tectonic and diagenetic fractures are developed in the tight gas sandstones of the Xujiahe Formation (T_3x) in the Jiulongshan gas field, China. The tectonic shear fractures are the main fracture type. Tectonic

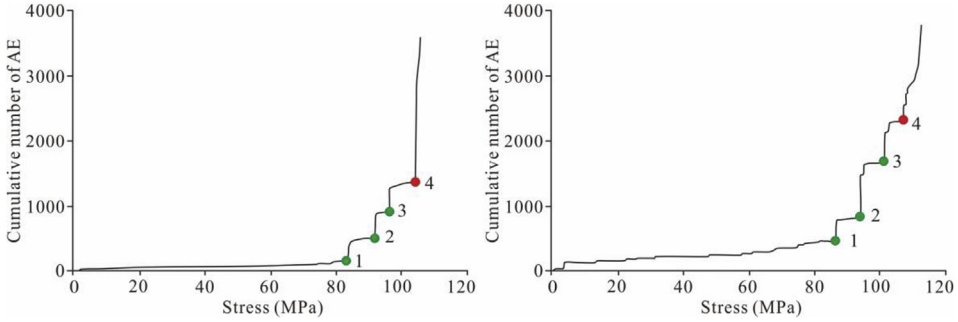

Fig. 10. Response curve of rock acoustic emission tests of the Xujiahe Formation (T_3x).

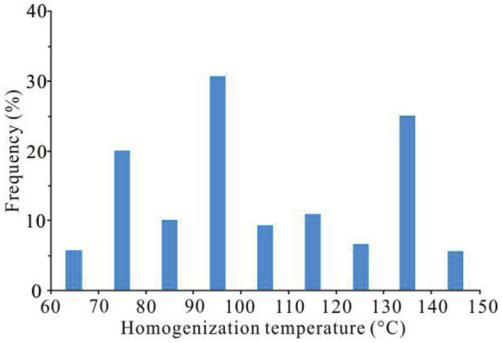

Fig. 11. The distribution of fluid inclusion homogenization temperatures from tectonic fractures of the Xujiahe Formation (T_3x).

fractures can be subdivided into steep fractures and nearly horizontal fractures according to their dip angles. These steep fractures and horizontal fractures interlace together and form prolific fracture networks, making the wells drilled in those areas are very productive. Diagenetic fractures usually develop along the bedding planes, and they are generally closed under the lithostatic pressure of the overlying strata. Three sets of tectonic fractures can be detected in the Xujiahe Formation (T_3x), namely: NW-SE trending, NNE-SSW trending, and NEE-SWW trending. The fracture heights measured from cores and outcrops are mainly distributed between 20 cm and 50 cm. The average fracture density of the steep fractures is 0.58 m^{-1}, and it varies distinctly in

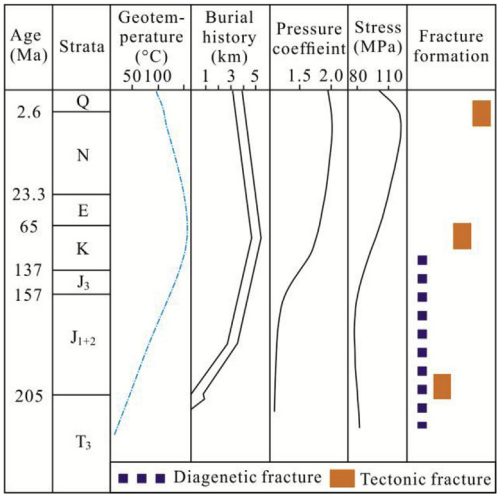

Fig. 13. Schematic map shows natural fracture sequences in the Xujiahe Formation (T_3x) at Jiulongshan gas field.

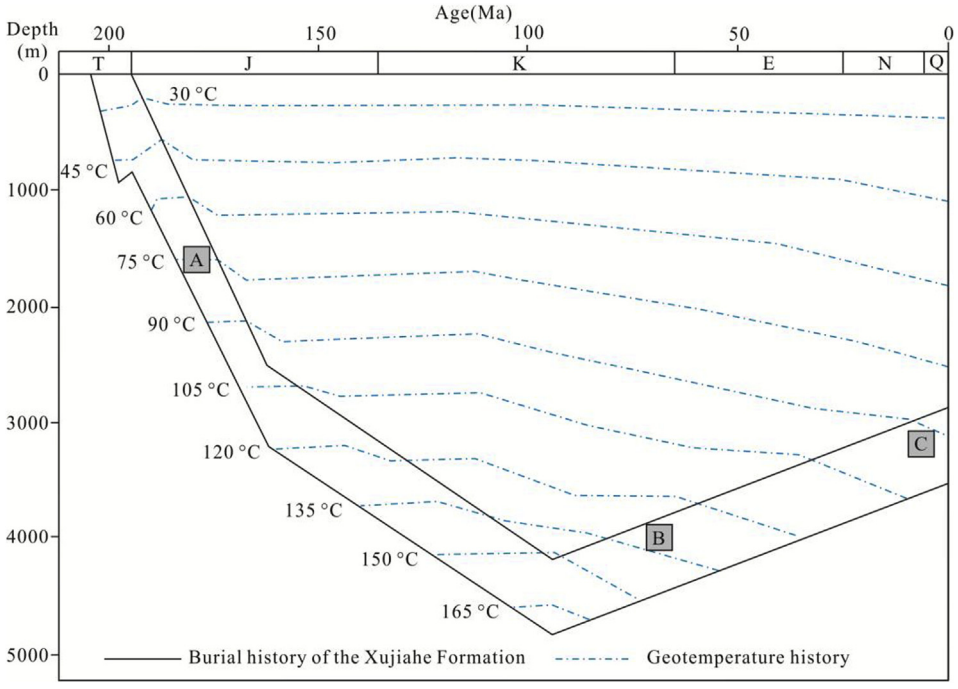

Fig. 12. Burial history, geo-temperature history and fracture filling events in the Xujaihe Formation (T_3x) of Jiulongshan gas Field.

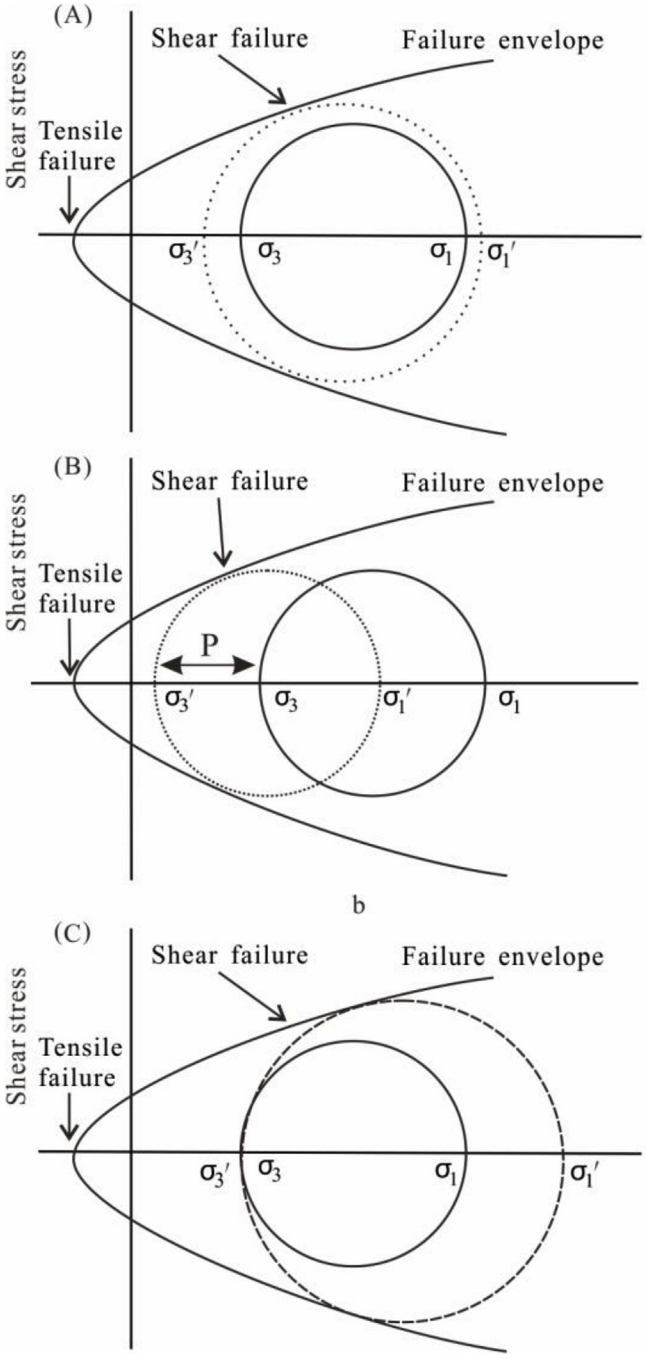

Fig. 14. Sketch map of tectonic fracture formation mechanism (Modified from Zeng, 2010).

different tectonic position and layers.

Based on the characteristics of fracture sets, crosscutting relationships, acoustic emission tests and fluid inclusion analysis, four periods of fractures can be identified in the study area. The first period is the diagenetic fractures which is formed under the intense compaction and dissolution from Late Triassic to Early Cretaceous. All the other three periods of fractures are tectonic fractures. Their formation time were at the end of the Triassic to the Early Jurassic, the Late Cretaceous and the end of Pliocene to the early of Pleistocene, respectively. Horizontal tectonic compression came from Longmenshan thrust belt and Micangshan uplift, abnormal high fluid pressure caused by deep burial and tectonic uplift are the mainly force sources for the formation of the steep fractures. The formation of nearly horizontal tectonic fractures is mainly related with the thrusting or inter-formational sliding caused by tectonic compression.

Acknowledgements

We thank Benjian Zhang and Hualing Ma at Northwest Sichuan Gas Field for their constructive help. This work was financially supported by the China Postdoctoral Science Foundation (grant nos. 2018M631908 and 2015M581424), National Natural Science Foundation of China (grant nos. 41502124 and U1562214), Natural Science Foundation of Heilongjiang Province (grant no. QC2018043), Young Innovative Talents Training Program for Universities in Heilongjiang Province (grant no. UNPYSCT-2018043), Cultivating Fund of Northeast Petroleum University (grant nos. SCXHB201705 and 2017PYQZL-14) and Young Science Foundation of Northeast Petroleum University (grant no. 2018QNL-12).

Appendix A. Supplementary data

Supplementary data to this article can be found online at https://doi.org/10.1016/j.petrol.2019.01.021.

References

Ameen, M.S., MacPherson, K., Al-Marhoon, M.I., Rahim, Z., 2012. Diverse fracture properties and their impact on performance in conventional and tight-gas reservoirs, Saudi Arabia: the Unayzah, South Haradh case study. AAPG (Am. Assoc. Pet. Geol.) Bull. 96 (3), 459–492.

Agosta, F., Wilson, C., Aydin, A., 2015. The role of mechanical stratigraphy on normal fault growth across a Cretaceous carbonate multi-layer, central Texas (USA). Italian J. Geosci. 134 (3), 423–441.

Bai, B., Zou, C., Zhu, R., Zhang, J., Tan, J., Zhang, B., Yang, H., Cui, J., Su, L., 2012. Characteristics and formation stage-times of structural fractures in tight sandstone reservoir of the 2nd Member of Xujiahe Formation in southwestern Sichuan Basin. Acta Geol. Sin. 86 (11), 1841–1846.

Cao, C., 2005. Tectonic Stress Field Analysis and Application in the Northwest Sichuan Basin. China geological academy of sciences.

Casini, G., Hunt, D.W., Monsen, E., Bounaim, A., 2016. Fracture characterization and modeling from virtual outcrops. AAPG (Am. Assoc. Pet. Geol.) Bull. 100 (1), 41–61.

Ding, Y., Zhang, D., 1991. Application of the incomplete erasion phenomenon in acoustic emission activities to the measurement of geostresses. Chin. J. Rock Mech. Eng. 10 (4), 313–326.

Ferrill, D.A., Mcginnis, R.N., Morris, A.P., Smart, K.J., Sickmann, Z.T., Bentz, M., Lehrmann, D., Evans, M.A., 2014. Control of mechanical stratigraphy on bed-restricted jointing and normal faulting: eagle Ford formation, south-central Texas. AAPG (Am. Assoc. Pet. Geol.) Bull. 98 (11), 2477–2506.

Ferrill, D.A., Morris, A.P., McGinnis, R.N., Smart, K.J., Wigginton, S.S., Hill, N.J., 2017. Mechanical stratigraphy and normal faulting. J. Struct. Geol. 94, 275–302.

Ge, X., Fan, Y., Zhu, X., Deng, S., Wang, Y., 2014. Reservoir fracture development using conventional well logging data—an application of kernel principal component analysis (KPCA) and multifractal detrended fluctuation analysis (MFDFA). IEEE J. Select. Topic. Appl. Earth Obs. Remote Sens. 7 (12), 4972–4978.

Ge, X., Fan, Y., Li, J., Zahid, M.A., 2015. Pore structure characterization and classification using multifractal theory—an application in Santanghu basin of western China. J. Petrol. Sci. Eng. 127, 297–304.

Gong, L., Gao, S., Fu, X., Chen, S., Lyu, B., Yao, J., 2017. Fracture characteristics and their effects on hydrocarbon migration and accumulation in tight volcanic reservoirs: a case study of the Xujiaweizi fault depression, Songliao Basin, China. Interpretation 5 (4), 57–70.

Gong, L., Zeng, L., Gao, Z., Zhu, R., Zhang, B., 2016. Reservoir characterization and origin of tight gas sandstones in the upper Triassic Xujiahe Formation, western Sichuan Basin, China. J. Petrol. Explor. .Product. Technol. 6 (3), 319–329.

Gong, L., Zeng, L., Du, Y., Han, Z., 2015. Influences of structural diagenesis on fracture effectiveness: a case study of the Cretaceous tight sandstone reservoirs of Kuqa foreland basin. J. China Inst. Min. Technol. 44 (3), 514–519.

Gong, L., Zeng, L., Pei, S., Zhang, B., Gao, Z., Zu, K., Li, H., 2013. Characteristics and origin of fractures in tight sandstone reservoirs of the second Member of Xujiahe Formation in Jiulongshan structure. Chin. J. Geol. 48 (1), 217–226.

He, P., Wang, Y., Liu, S., Zhou, W., 1999. Multi-information coincidence evaluation fracture of Xu2 lower section gas pool in Jiulongshan gas field. J. Chengdu Univ. Technol. 26 (3), 225–227.

Hooker, J.N., Laubach, S.E., Marrett, R., 2013. Fracture-aperture size-frequency, spatial distribution, and growth processes in strata-bounded and non-strata-bounded fractures, Cambrian Mesón Group, NW Argentina. J. Struct. Geol. 54, 54–71.

Kong, L., Ostadhassan, M., Li, C., Tamimi, N., 2018. Pore characterization of 3D-printed gypsum rocks: a comprehensive approach. J. Mater. Sci. 53 (7), 5063–5078.

Larsen, B., Grunnaleite, I., Gudmundsson, A., 2010. How fracture systems affect permeability development in shallow-water carbonate rocks: an example from the Gargano

Peninsula, Italy. J. Struct. Geol. 32 (9), 1212–1230.
Laubach, S.E., Eichhubl, P., Hilgers, C., Lander, R.H., 2010. Structural diagenesis. J. Struct. Geol. 32 (12), 1866–1872.
Laubach, S.E., Olson, J.E., Gross, M.R., 2009. Mechanical and fracture stratigraphy. AAPG Bull. 93 (11), 1413–1426.
Laubach, S.E., Fall, A., Copley, L., Marrett, R., Wilkins, S.J., 2016. Fracture porosity creation and persistence in a basement-involved Laramide fold, upper cretaceous frontier formation, green river basin, USA. Geol. Mag. 153 (5–6), 887–910.
Liu, S., He, P., Deng, R., Pang, J., Zhan, T., 1996. Fracture distribution of Xu2 member in Jiulongshan structure of western Sichuan Basin. Nat. Gas. Ind. 16 (2), 1–4.
Liu, H., Liang, H., Cai, L., Shen, F., 1994. Structural styles of the Longmenshan thrust belt and evolution of the foreland basin in western Sichuan province, China. Acta Geol. Sin. 68 (2), 101–118.
Luo, Q., Gong, L., Qu, Y., Zhang, K., Zahng, G., Wang, S., 2018. The tight oil potential of the Lucaogou formation from the southern Junggar Basin, China. Fuel 234, 858–871.
Lyu, W., Zeng, L., Liu, Z., Liu, G., Zu, K., 2016. Fracture responses of conventional logs in tight-oil sandstones: a case study of the Upper Triassic Yanchang Formation in southwest Ordos Basin, China. AAPG (Am. Assoc. Pet. Geol.) Bull. 100 (9), 1399–1417.
Lyu, W., Zeng, L., Zhang, B., Miao, F., Lyu, P., Dong, S., 2017. Influence of natural fractures on gas accumulation in the Upper Triassic tight gas sandstones in the northwestern Sichuan Basin, China. Mar. Petrol. Geol. 83, 60–72.
Marrett, R., Gale, J.F.W., Gómez, L.A., Laubach, S.E., 2018. Correlation analysis of fracture arrangement in space. J. Struct. Geol. 108, 16–33.
Olson, J.E., Laubach, S.E., Eichhubl, P., 2010. Estimating natural fracture producibility in tight gas sandstones: coupling diagenesis with geomechanical modeling. Lead. Edge 29 (12), 1494–1499.
Pei, S., Dai, H., Yang, Y., Li, Y., Duan, Y., 2008. Evolutionary characteristics of T3x2 reservoir in Jiulongshan structure, northwest Sichuan basin. Nat. Gas. Ind. 28 (2), 51–53.
Petrie, E.S., Evans, J.P., Bauer, S.J., 2014. Failure of cap-rock seals as determined from mechanical stratigraphy, stress history, and tensile-failure analysis of exhumed analogs. AAPG (Am. Assoc. Pet. Geol.) Bull. 98 (11), 2365–2389.
Procter, A., Sanderson, D.J., 2018. Spatial and layer-controlled variability in fracture networks. J. Struct. Geol. 108, 52–65.
Qiu, Z., He, P., 1990. Analysis of the controlling factors of the commercial gas wells in Xu2 reservoir in Jiulongshan gas field. Nat. Gas. Ind. 10 (4), 7–10.
Sanderson, D.J., Nixon, C.W., 2015. The use of topology in fracture network characterization. J. Struct. Geol. 72, 55–66.
Smart, K.J., Ofoegbu, G.I., Morris, A.P., McGinnis, R.N., Ferrill, D.A., 2014. Geomechanical modeling of hydraulic fracturing: why mechanical stratigraphy, stress state, and pre-existing structure matter. AAPG (Am. Assoc. Pet. Geol.) Bull. 98 (11), 2237–2261.
Wang, L., Zhao, N., Sima, L., Meng, F., Guo, Y., 2018a. Pore structure characterization of the tight reservoir: systematic integration of mercury injection and nuclear magnetic resonance. Energy Fuels 32 (7), 7471–7484.
Wang, X., Hou, J., Song, S., Wang, D., Gong, L., Ma, K., Liu, Y., Li, Y., Yan, L., 2018b. Combining pressure-controlled porosimetry and rate-controlled porosimetry to investigate the fractal characteristics of full-range pores in tight oil reservoirs. J. Petrol. Sci. Eng. 171, 353–361.
Yu, H., Zhou, W., 2001. A research on distribution law of fracture in Xujiahe Formation in Songhua-Baima region. J. Chengdu Univ. Technol. 28 (2), 174–178.
Yuan, Q., Li, B., Liu, H., Liu, S., Wang, L., 2010. The tectonics evolution and lithofacies palaeogeography in the northwest of the Sichuan basin. J. Daqing Pet. Inst. 34 (6), 42–52.
Zeng, L., 2010. Microfracturing in the Upper Triassic Sichuan Basin tight gas sandstones: tectonic, overpressuring, and diagenetic origins. AAPG (Am. Assoc. Pet. Geol.) Bull. 94 (12), 1811–1825.
Zeng, L., Li, Y., 2010. Tectonic fractures in the tight gas sandstones of the upper Triassic Xujiahe Formation in the western Sichuan Basin, China. Acta Geol. Sin. 84 (5), 1229–1238.
Zeng, L., Tang, X., Wang, T., Gong, L., 2012. The influence of fracture cements in tight Paleogene saline lacustrine carbonate reservoirs, Western Qaidam Basin, Northwest China. AAPG (Am. Assoc. Pet. Geol.) Bull. 96 (11), 2003–2017.
Zhao, P., Cai, J., Huang, Z., Ostadhassan, M., Ran, F., 2018. Estimating permeability of shale gas reservoirs from porosity and rock compositions. Geophysics 83 (5), 1–36.